Solution of the Neumann Pressure Problem in General Orthogonal Coordinates Using the Multigrid Technique

U. Ghia,* R. Ramamurti,† and K. N. Ghia‡
University of Cincinnati, Cincinnati, Ohio

The multigrid (MG) technique has been advanced for use with Neumann boundary-value problems in clustered curvilinear orthogonal coordinates. This comprises an important step in the analysis of incompressible flow using the velocity-pressure formulation of the Navier-Stokes equations. The finite-difference representation of the problem and the formulation of the restriction and coarse-grid correction operators are examined in detail. Maintaining consistency between these and the integral constraint associated with the Neumann problem is found to be critical for the success of the MG technique. The influence of the smoothing operator is examined by employing Gauss-Seidel, alternating-direction implicit, and strongly implicit techniques. The MG procedure enhances the efficiency of fine-grid solutions of the Neumann problem by a factor of 3 to 14, depending on the type of smoothing operator employed and the values of the problem parameters.

I. Introduction

VELOCITY-PRESSURE formulations of the equations governing incompressible viscous flows generally require the solution of a Neumann boundary-value problem for the determination of pressure.[1-5] A peculiarity of the Neumann problem is that associated with it is an integral constraint relating the source distribution and the boundary values of the problem. Exact satisfaction of this constraint is necessary for the existence of a steady-state solution. In the framework of a finite-difference solution procedure, the discretized form of this constraint must be satisfied by the finite-difference equations in order for the procedure to lead to a converged numerical solution. Even for the constant-coefficient case that occurs in Cartesian coordinates, differences in the truncation errors due to discretization of various terms can prevent the required integral constraint from being satisfied exactly. In the more general cases with nonconstant coefficients that occur in curvilinear orthogonal coordinates and when grid-clustering coordinate transformations are employed, inconsistencies in discretization may contribute an additional discrepancy in the satisfaction of the integral constraint. In all circumstances, this discrepancy must be compensated for by modifying the source distribution in order to guarantee convergence. It is, therefore, necessary to minimize this discrepancy in order to minimize modification of the original problem.

In several flow configurations, particularly those at high Reynolds number, solutions are needed on a highly refined mesh in order to predict accurately the detailed features of the prevailing flow pattern. Conventional iterative methods such as successive overrelaxation (SOR), alternating-direction implicit (ADI), and strongly implicit (SI) are known to exhibit unsatisfactory convergence behavior for these fine-mesh solutions after the initial few iterations. The multigrid (MG) technique[6] has now been adequately demonstrated to lead to considerable convergence enhancement for flow problems such as the asymptotic curved-duct flow[7] and the driven cavity flow[8] for Re as high as 10,000 and grids as fine as 257×257. In both of these efforts, the MG procedure enabled acceleration of the convergence rate by a factor of at least four for configurations with extreme values of the problem parameters. For moderate values of the problem parameters, higher gains in convergence rate were observed.

The present study examines the solution of a two-dimensional Neumann boundary-value problem using the MG technique. Even for problems with constant coefficients, the MG solution procedure is not very straightforward. Extension to the Neumann boundary-value problem with nonconstant coefficients requires further careful considerations. These arise from the following. On the finest grid, a converged solution is ensured, since any discrepancy in satisfying the integral constraint may be compensated for by uniform modification of the source term. Thereafter, no modification should be made on any of the subsequent grids. Nevertheless, even on these coarser grids, the integral constraint should be satisfied in a natural manner. Failure to do so results in slow convergence and leads, eventually, to numerical instability. In the present study, the integral constraint on the coarser grids is satisfied via appropriate definition of the restriction operator. This operator is examined in detail in relation to the integral constraint on consecutive fine and coarse grids, and its appropriate form has been derived. Special forms of this operator are obtained for the boundaries and corners of the solution domain.

II. Formulation of Neumann Boundary-Value Problem

In a velocity-pressure representation of the Navier-Stokes equations, the elliptic problem for pressure is formulated by forming the divergence of the momentum equations. With intended application to duct flows, the configurations considered in the present study correspond to parabolic flow through straight and curved ducts of simple rectangular or polar cross sections. These configurations have been studied earlier by K. Ghia, U. Ghia, and their co-workers. In particular, the formulation used here follows that of Ghia et al.,[5] who also employed grid-clustering coordinate transformations to re-

Presented as AIAA Paper 83-0557 at the AIAA 21st Aerospace Sciences Meeting, Reno, NV, Jan. 10-13, 1983; received May 1, 1987, revision received Dec. 29, 1987.

*Professor, Department of Mechanical and Industrial Engineering. Associate Fellow AIAA.

†Research Associate, Department of Aerospace Engineering and Engineering Mechanics. Member AIAA.

‡Professor, Department of Aerospace Engineering and Engineering Mechanics. Associate Fellow AIAA.

solve the high-gradient regions normal to the duct walls. With the nomenclature used in Ref. 5, the (ξ,η) cross-plane momentum equations may be represented as

$$\xi' \frac{\partial p}{\partial \xi} = F_1 \tag{1a}$$

$$\frac{1}{r^m}\eta' \frac{\partial p}{\partial \eta} = F_2 \tag{1b}$$

where p is the cross-plane pressure; ξ,η denote computational cross-plane coordinates corresponding to (x,y) or (r,θ), with primes denoting differentiation; $m = 0$ for rectangular cross-section ducts, $m = 1$ for circular cross-section ducts, and F_1, F_2 represent all the velocity terms in the momentum equations.

The details of the expressions for F_1 and F_2 are not relevant for the purpose of the present study and are, therefore, not given here; they are available in Ref. 5. For the parabolic duct-flow configuration considered, the cross-plane Laplacian operator is defined as

$$\nabla^2 = \xi'^2 \frac{\partial^2}{\partial \xi^2} + \xi'' \frac{\partial}{\partial \xi} + \frac{m}{r}\xi' \frac{\partial}{\partial \xi} + \frac{1}{r^{2m}}\left[\eta'^2 \frac{\partial^2}{\partial \eta^2} + \eta'' \frac{\partial}{\partial \eta}\right] + \frac{n}{(R + rc^m)}\left[c^m \xi' \frac{\partial}{\partial \xi} - \frac{ms}{r}\eta' \frac{\partial}{\partial \eta}\right] \tag{2}$$

where $n = 0$ for straight ducts and $n = 1$ for curved ducts, R = radius of longitudinal curvature, $c = \cos\theta$, and $s = \sin\theta$. Therefore, the pressure equation is obtained as

$$\nabla^2 p = S_p \tag{3}$$

where

$$S_p = \xi' \frac{\partial F_1}{\partial \xi} + \frac{\xi' F_1}{r^m (R^n + nrc^m)} \frac{\partial}{\partial \xi}\left[r^m (R^n + nrc^m)\right] + \frac{\eta'}{r^m}\frac{\partial F_2}{\partial \eta} + \frac{n\eta' F_2}{(R^n + nrc^m)} \frac{\mathrm{d}}{\mathrm{d}\eta}\left[c^m\right] \tag{4}$$

Equation (3) is a Poisson equation for pressure. The boundary conditions required for its solution are obtained by evaluating the normal gradients of pressure at the problem boundaries using Eqs. (1). Hence, Eqs. (1) and (3) constitute a Neumann boundary-value problem for pressure.

Frequently, the distribution of the source function [S_p in Eq. (3)] and the boundary functions [F_1 and F_2 in Eqs. 1] can influence the convergence behavior of the numerical solutions. This is, indeed, confirmed by also considering the Neumann problem obtained for a correction-velocity potential Φ with source function S_Φ and homogeneous Neumann boundary values. The significance of the function Φ as well as the details of this Neumann problem are described in Ref. 9.

The considerations required for obtaining a convergent solution to Neumann problems using a single grid (SG) have been discussed in Ref. 5 and are summarized in Sec. III.

III. Remarks on Single-Grid Solution of Neumann Problems

A unique property of the Neumann problem is that the Laplacian operator in the governing differential equation and the normal-derivative operator in the boundary values are related via the Gauss divergence theorem. Consequently, the source function S and the boundary-value function G are also similarly related by the integral theorem

$$\iint_A S\, \mathrm{d}A = \int_C G\, \mathrm{d}\eta \tag{5}$$

where C is the closed curve bounding the solution domain A. Failure to satisfy Eq. (5) will cause eventual divergence of the resulting solution. Generally, Eq. (5) may not be satisfied exactly due to differences in truncation errors of discretization of the various terms in S and G. In order to ensure convergence, it is necessary to define a modified source function S' as

$$S' = S - \frac{\epsilon}{A} \tag{6}$$

where

$$\epsilon = \iint_A S\, \mathrm{d}A - \int_C G\, \mathrm{d}n \tag{7}$$

i.e., ϵ represents a measure of the extent to which the discretized version of Eq. (5) is not satisfied. Then, with S replaced by S', Eq. (5) is satisfied exactly.

The integral constraint (5) associated with the Neumann problem also implies some requirements on the discretization process. First of all, the ∇^2 operator must be in the conservation form as far as possible. Second, the form of the equation solved at each computational point must be guided by the form in which S appears in Eq. (5). Accordingly, the pressure equation, for example, must be written at each computational point as

$$\sum_{i=1}^{I} a_i \nabla_i^2 p = \sum_{i=1}^{I} a_i S_{p_i} \tag{8}$$

where $a = r^m[R^n + nrc^m]/(\xi'\eta')$; $I = 4$ at general interior points, 2 at general boundary points, and 1 at corner points; and i refers to the center of cells adjoining the computational point under consideration. Also, the subscript i on ∇^2 and S denotes that coefficients in these quantities are to be evaluated at the four possible positions indicated as $(r \pm \Delta r/2, \theta \pm \Delta\theta/2)$. The conservation form of $\nabla^2 p$ requires that, in defining Eq. (2), ξ'', η'' and s ($= \sin\theta$) have the following representation:

$$\xi'' = \frac{\mathrm{d}(\xi')}{\mathrm{d}\xi}\xi' \tag{9a}$$

$$\eta'' = \frac{\mathrm{d}(\eta')}{\mathrm{d}\eta}\eta' \tag{9b}$$

$$\sin\theta = -\frac{\mathrm{d}}{\mathrm{d}\eta}(\cos\theta)\,\eta' \tag{9c}$$

With this formulation of the discretized Neumann problem and the SOR technique, Ghia and co-workers[5] had obtained rapidly converging solutions for p and Φ for laminar flow through curved polar ducts using 21×21 grids with ξ'_{wall}, $\eta'_{\text{wall}} \approx 2$, i.e., with the near-wall increment of approximately 1/40. For the corresponding turbulent flow, which requires better resolution of the near-wall region, Goyal et al.[10] had experienced considerably slower convergence rates for the SOR procedure using finer grids. Hence, in the present investigation we use the MG technique for convergence acceleration.

IV. Application of MG Technique

The MG technique[6] is a numerical strategy for enhancing the convergence rate of an iterative procedure. The discretized problems corresponding to Eq. (3) subject to Neumann boundary conditions can be solved using a conventional iterative technique. Generally, the convergence of these schemes is fast during the first few iterations only, and is effective only on those Fourier components of the error whose wavelengths are smaller than or comparable to the grid increment. The more slowly varying components of the error are rather slow in being annihilated. The MG method recognizes that a wavelength that is long relative to a fine mesh

is short relative to a coarser mesh. It employs a hierarchy of grids D^k, $k = 1,2,\ldots,M$, with mesh width h_k such that $h_{k+1} = h_k/2$. When the convergence rate of the solution on the fine grid becomes slow, the MG procedure switches to a coarser grid, where the longer wavelength errors are more effectively damped. The solution on the finer grid is then corrected appropriately to reflect the removal of these long wavelength Fourier components of the error. Brandt[6] has detailed the several possibilities that present themselves in the development of the MG procedure. In any MG method, a choice has to be made for the basic iterative scheme to be used for high-frequency error damping, i.e., for smoothing the error. Operators need to be defined for transferring the error from the fine grid to the coarse grid (restriction operator) and for transferring the correction from the coarse grid to the fine grid (prolongation operator). Further, convergence and convergence rate need to be defined. Brandt[6] has provided guidelines for dealing with these and other issues pertinent to the MG process. Ghia and co-workers[7,8] have applied Brandt's guidelines and investigated them further, specifically in relation to the solution of Navier-Stokes equations formulated in terms of vorticity and stream function, i.e., not involving a Neumann problem. The details outlined here are primarily the additional considerations needed for the MG solution of Neumann problems.

In the MG solution of a Neumann problem, a convergent solution on the finest grid is ensured when the measures described in Sec. III are observed. No further modification of the problem may be made on the subsequent coarse grids. On these grids, convergence must be obtained by appropriately formulating the coarse-grid problems to satisfy automatically the integral constraint [Eq. (5)] on all coarse grids.

Formulation of Coarse-Grid Problem

This involves, first of all, the derivation of a suitable restriction operator R_k^{k-1}. This derivation is guided by the discretized representation of the integral constraint [Eq. (5)]. This integral constraint can be satisfied automatically on the coarser grid if the area integral and the line integral on a fine grid are made individually equal to the corresponding area integral on a subsequent coarse grid. To achieve this, it is useful to refer to the sketch in Fig. 1a for a typical computational region; here, numerals designate fine-grid points, while letters designate coarse-grid points. The Neumann problem to be solved [Eq. (8)] for pressure may be represented symbolically on the fine grid as

$$L^f p = S^f \tag{10}$$

with the boundary conditions

$$B^f p = G^f \tag{11}$$

Then, using the trapezoidal rule of integration, the area integral of S on the fine grid can be written as

$$\begin{aligned} AI^f = {} & \mathrm{d}A^f \cdot [(1/4)(S_1^f + S_5^f + S_{21}^f + S_{25}^f) \\ & + (1/2)(S_2^f + S_3^f + S_4^f + S_6^f + S_{11}^f + S_{16}^f + S_{10}^f \\ & + S_{15}^f + S_{20}^f + S_{22}^f + S_{23}^f + S_{24}^f) \\ & + (S_7^f + S_8^f + S_9^f + S_{12}^f + S_{13}^f + S_{14}^f + S_{17}^f + S_{18}^f + S_{19}^f)] \end{aligned} \tag{12}$$

where $\mathrm{d}A^f$ is the elemental fine-grid area. Similarly, the area integral on a subsequent coarse grid can be written as

$$\begin{aligned} AI^c = {} & \mathrm{d}A^c \cdot [(1/4)(S_A^c + S_C^c + S_G^c + S_I^c) \\ & + (1/2)(S_B^c + S_D^c + S_H^c + S_F^c) + S_E^c] \end{aligned} \tag{13}$$

where $\mathrm{d}A^c$ is the elemental coarse-grid area. With a mesh width ratio $h_{k+1}/h_k = 1/2$,

$$\mathrm{d}A^c = 4\ \mathrm{d}A^f \tag{14}$$

Also, S^c represents the coarse-grid source term obtained by restriction of the fine-grid source term as

$$S^c = R_k^{k-1} S^f \tag{15}$$

Comparison of Eqs. (12) and (13), together with the use of Eq. (14), suggests that, for AI^f to be equal to AI^c, the restriction operator R_k^{k-1} must be defined such that the coarse-grid source term is related to the fine-grid source as follows.

At a general interior point, S^c is a 9-point average of S^f, e.g.,

$$\begin{aligned} S_E^c = {} & (1/4)S_{13}^f + (1/8)(S_8^f + S_{12}^f + S_{14}^f + S_{18}^f) \\ & + (1/16)(S_7^f + S_9^f + S_{17}^f + S_{19}^f) \end{aligned} \tag{16}$$

This corresponds to full-weighted averaging introduced by Brandt[6] and is the same as the 9-point restriction used by Wesseling.[11]

At a general boundary point, S^c is a 6-point average of S^f, e.g.,

$$S_B^c = (1/4)(S_3^f + S_8^f) + (1/8)(S_2^f + S_4^f + S_7^f + S_9^f) \tag{17}$$

Equation (17) may be viewed as a specialization of the general Eq. (16), by eliminating the influence of the three fine-grid points that lie beyond the boundary and doubling the influence of the three fine-grid interior points.

At a corner, S^c is formed as a 4-point average of S^f, e.g.,

$$S_A^c = (1/4)(S_1^f + S_2^f + S_6^f + S_7^f) \tag{18}$$

Again, Eq. (18) may be viewed as a specialization of Eq. (17) applied to a corner point.

The weighted-averaging operators defined by Eqs. (16–18) are represented in Figs. 1b–1d, respectively.

Next, attention is directed toward the line integral of the boundary values G. In the fine grid, this is represented, again using trapezoidal rule, as

$$\begin{aligned} I^f = {} & \mathrm{d}s^f \cdot [(1/2)(G_{1_\xi}^f + G_{5_\xi}^f + G_{21_\xi}^f + G_{25_\xi}^f + G_{1_\eta}^f + G_{5_\eta}^f \\ & + G_{21_\eta}^f + G_{25_\eta}^f) + (G_2^f + G_3^f + G_4^f + G_6^f + G_{11}^f + G_{16}^f + G_{10}^f \\ & + G_{15}^f + G_{20}^f + G_{22}^f + G_{23}^f + G_{24}^f)] \end{aligned} \tag{19}$$

where $\mathrm{d}s^f$ is the incremental length on the fine-grid boundary. Similarly, the line integral of the boundary values on the coarse grid is represented as

$$\begin{aligned} I^c = {} & \mathrm{d}s^c \cdot [(1/2)(G_{A_\xi}^c + G_{C_\xi}^c + G_{G_\xi}^c + G_{I_\xi}^c + G_{A_\eta}^c + G_{C_\eta}^c \\ & + G_{G_\eta}^c + G_{I_\eta}^c) + (G_B^c + G_D^c + G_F^c + G_H^c)] \end{aligned} \tag{20}$$

where $\mathrm{d}s^c$ is the line increment along the coarse-grid boundary and, with a mesh-width ratio of 1/2,

$$\mathrm{d}s^c = 2\ \mathrm{d}s^f \tag{21}$$

Comparison of Eqs. (19) and (20), together with use of Eq. (21), suggests that $I^c = I^f$ if the coarse-grid boundary values are related to the fine-grid boundary values as follows.

At a general boundary point, such as D, a 3-point average must be employed, e.g.,

$$G_D^c = (1/4)\ G_6^f + (1/2)G_{11}^f + (1/4)\ G_{16}^f \tag{22}$$

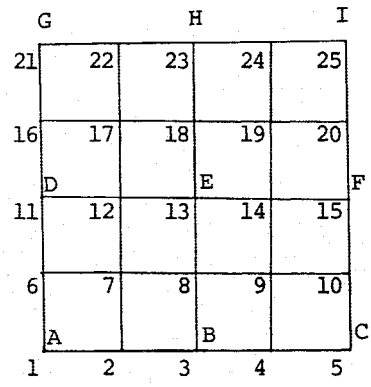

Fig. 1a Grid nomenclature used in Sec. IV.

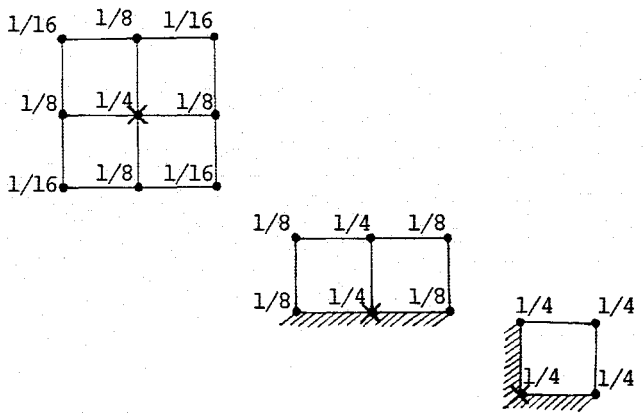

Fig. 1b Weighting factors for restriction operators: a) interior point, b) general boundary point, and c) corner point.

At a corner, such as A, a simple 2-point average is employed, e.g.,

$$G_A^c = (1/2)(G_1^f + G_2^f) \tag{23}$$

Equations (22) and (23) may be viewed as one-dimensional analogs of Eqs. (16–18).

The restriction operators defined by Eqs. (16–18), (22), and (23) must be used to define the coefficients of the various terms in the differential operator in the coarse-grid-correction equation. Accordingly, the discretized coarse-grid operators are of the same form as the corresponding fine-grid operators, with the coefficients of the former derived from the coefficients of the latter using expressions of the form given by Eqs. (16–18), (22), and (23).

Outline of MG Procedure Used

Since the Neumann problem represented by Eq. (8) is linear, the Correction-Storage (CS) algorithm[6] is used. The procedure is started with an approximate solution on the finest grid. In the terminology of Brandt,[6] this then corresponds to the CS-cycle C algorithm. The initial guess for the solution on the finest grid may consist of a constant distribution for the first computational plane of the duct. For successive planes, the solution at the preceding plane comprises a good starting solution. The basic steps of the MG algorithm used to obtain a converged solution are outlined next.

1) The solution on the finest grid is relaxed (or smoothed) using a selected smoothing operator to relax Eqs. (10) and (11). Concurrent with the process of relaxation, a suitable norm of the residuals of Eq. (10) is computed. The norm usually used is the L_2 norm defined as

$$e_{k+1}^q = \| S^{k+1} - L^{k+1} p^{k+1,q} \| \tag{24}$$

where $p^{k+1,q}$ is the solution after q relaxation sweeps, and $(k+1)$ corresponds to the finest grid M.

2) The residual norm e_{k+1}^q is compared with a prescribed tolerance ϵ_{k+1} (taken to be 10^{-7} for the finest grid in the present work). If $e_{k+1}^q \le \epsilon_{k+1}$, convergence has been achieved, and the solution procedure is terminated. If $e_{k+1}^q > \epsilon_{k+1}$, then the convergence rate, defined as $e_{k+1}^q / e_{k+1}^{q-1}$, is computed and compared with a prescribed value ζ, which is related to the smoothing rate of the relaxation operator used. If the observed convergence rate is smaller than ζ, the relaxation continues; otherwise, the procedure switches to a coarser grid, if the present grid is not the coarsest.

3) The coarse grid-correction equation is defined as

$$L^k p^k = S^k \tag{25}$$

where

$$S^k = R_{k+1}^k (S^{k+1} - L^{k+1} p^{k+1}) \tag{26}$$

for the CS algorithm, and R_{k+1}^k is the restriction operator obtained in the preceding section. It is also necessary to note that, in a Neumann problem, a nonzero residual exists in the boundary conditions at those boundaries that are treated explicitly in the relaxation process. Accordingly, nonzero boundary-value residuals are involved at all boundaries with the explicit SOR iteration procedure. On the other hand, the SI procedure that treats all boundary conditions implicitly involves zero boundary-value residuals at all boundaries. The tolerance for the problem on grid D^k is set as

$$\epsilon_k = \delta \, e_{k+1} \tag{27}$$

where δ varies between 0.2 and 0.5. Convergence and convergence rate are monitored as described in step 2. If slow convergence is observed, the process switches to a yet coarser grid. If the coarse-grid residual norm $e_k \le \epsilon_k$ defined in Eq. (27), the process switches to the finer grid. On the coarsest grid used, convergence must be obtained; the specific relaxation operator used may have a significant role in achieving this.

4) The coarse-grid correction is employed to improve the solution on the fine grid according to the relation

$$p_{\text{new}}^{k+1} = p_{\text{old}}^{k+1} + P_k^{k+1} p^k \tag{28}$$

where P_k^{k+1} is the 9-point prolongation operator based on linear interpolations.

Steps 1–4 are repeated until convergence is achieved on the finest grid. The procedure outlined above is adaptive, in the sense that internal checks dictate the switching between the coarse and the fine grids, based on pre-assigned values of ζ and δ. A fixed MG procedure is one in which the internal checks are replaced by a pre-assigned number N^k of the iterations on grids D^k, where the value of N^k is also guided by the smoothing rate of the relaxation scheme. The main avdantage of fixed algorithms is the associated saving of computational effort, since convergence then needs to be checked only on the finest grid. In the present study, both adaptive and fixed algorithms were investigated. Their effects on the efficiency of the overall procedure, as well as the various other results obtained, are discussed in the next section.

V. Discussion of Results

The MG procedure outlined in the preceding section was used to solve the Neumann problems for the pressure p and the correction-velocity potential Φ for the developing flow through various duct configurations. The formulation of the

restriction operator and the coarse-grid-correction equation, as described in Sec. IV, and the correctness of the computer program were checked via application to the following model problem.

Model Problem

The boundary-value problem governed by a differential equation of the form given in Eq. (3) was formulated by starting with a known analytical function $F(r,\theta)$. The source term $S(r,\theta)$ is generated by operating on $F(r,\theta)$ with the discretized ∇^2 operator defined in Eq. (2). Similarly, the normal-derivative boundary value for the Neumann model problem is generated by forming the discretized normal derivative of $F(r,\theta)$ at the boundaries. It is important that both the source and the boundary conditions be evaluated using the finite-difference representation of the differential operators involved. If analytical differentiation of $F(r,\theta)$ is used to define the problem, then the finite-difference form of the integral constraint [Eq. (5)] will not be satisfied exactly. A nonzero modification [Eq. (6)] of the source term will then be required on the finest grid in order to ensure convergence of the solution. The converged solution of the problem with the modified source term will necessarily differ from the starting analytical solution. It will then not be possible to make any definitive statements regarding correctness of the present analysis.

With appropriate formulation of the source term and the boundary conditions, the present analysis and program were tested for various forms of the Laplacian operator, corresponding to different duct configurations, with uniform as well as clustered grids. Also, both Dirichlet and Neumann problems were examined. In all cases, the numerical solution obtained for $F(r,\theta)$ was identical to the starting analytical function. This provides reasonable credibility to the results presented in the remainder of the study.

Neumann Problems in Duct Flows

The analysis and solution procedure developed were then used to determine the developing flow in straight/curved ducts of rectangular/polar cross sections. The emphasis of the present study is not on the overall flow solution but on the efficient solution of the Neumann boundary-value problems encountered in the flow calculation. Hence, the majority of the results presented here pertain to the convergence history of the solutions for Φ and p for the duct cross sections. Also, the computational effort involved in obtaining these solutions is examined in detail. For this purpose, a cross plane located very near the entrance section of the duct has been selected because, in earlier single-grid studies of the problem, the slowest convergence rates were experienced in this region with large cross-flow gradients near the duct walls. Also, the influence of the relaxation or smoothing operator on the overall efficiency of the solution is examined by employing Gauss-Seidel (GS), ADI, and SI procedures as smoothing operators.

In the figures and tables presented, the duct configurations are denoted by a sequence of three uppercase letters. The first letter indicates whether the duct is straight (S) or curved (C). The second letter indicates whether the duct cross section is square (S) or polar (P). The last letter corresponds to uniform grids (U) or stretched grids (S). Thus, CPS corresponds to curved polar duct with grid stretching. Also, MG denotes multigrid solutions, SG denotes single-grid solutions, and GS denotes the Gauss-Seidel iterative procedure.

Results for Gauss-Seidel Relaxation

Multigrid solutions were obtained for various duct configurations with the finest grid consisting of 21×21 points, using a total of three grid levels. The number of fine-grid iterations required for the Φ and p solutions are listed in Table 1. On plane 3 for the simple SSU configuration, the MG procedure leads to a reduction in the iterations by a factor of 1.5, as compared to the conventional SOR procedure with the optimum relaxation factor ω_{opt}. This low a factor is caused by the MG procedure, which could be better optimized for this simple configuration, or by the high efficiency of the SOR scheme for the Poisson equation on a uniform Cartesian grid. Far downstream, i.e., on plane 100, the corresponding reduction factors are 5 and 10 for Φ and p, respectively. However, the gain observed in computer time for the complete solution up to 100 planes is only a factor of 1.5 because the MG procedure is used only for the solution of the Poisson

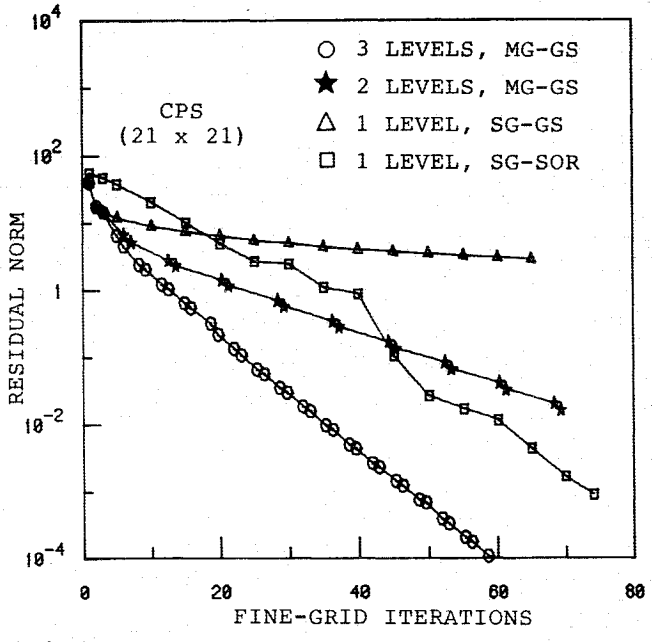

Fig. 2 Convergence history for GS, SOR, and MG-GS schemes: Φ equation, plane 3.

Table 1 Comparison of computational effort for MG-GS and SG-SOR schemes: finest grid, 21×21

Duct Configuration	MG-GS 3-levels ($\zeta = 0.6$)						SG-SOR					
	No. of iterations				CPU s (100 planes)	δ	No. of iterations				CPU s (100 planes)	ω_{opt}
	Plane 3		Plane 100				Plane 3		Plane 100			
	Φ	p	Φ	p			Φ	p	Φ	p		
SSU	41.2	44.6	4.9	1.0	203	0.3	67	66	26	10	340	1.805
SPU	34.8	37.2	4.9	1.0	209	0.3	76	74	24	7	363	1.805
CSU	41.1	44.6	32.0	9.9	265	0.3	68	61	65	26	387	1.805
CPU	40.7	46.4	31.8	15.7	271	0.3	64	78	53	17	380	1.805
SSS	50.5	51.1	4.0	1.0	215	0.3	70	62	72	75	371	1.845
SPS	58.6	67.0	5.4	1.0	228	0.3	82	79	79	75	387	1.845
CSS	58.9	65.5	51.3	25.1	333	0.37	79	79	68	43	398	1.845
CPS	61.8	69.0	51.3	20.4	337	0.35	79	79	67	48	400	1.845

equations, which are two of the five equations involved in the total solution procedure. As the problem complexity is increased via the introduction of the transverse or longitudinal curvature and grid clustering, the gain achieved using the MG technique, as compared to SG-SOR, becomes smaller. Thus, for the CPS configuration, the reduction factor for the Φ solution on plane 3 is only about 1.3. Hence, this case has been examined further in Fig. 2, which presents the convergence history for the Φ solution on plane 3. Starting with the single-grid Gauss-Seidel (SG-GS) scheme, the successive inclusion of one and two coarser grids in the MG-GS scheme shows a significant improvement in the rate of error reduction. However, the curve for the SG-SOR scheme lies between the two-level MG and the three-level MG schemes. The inclusion of yet another coarser grid may have improved the convergence rate further. But, with the finest grid of 21×21, the 6×6 grid is the coarsest grid possible with a mesh reduction of one-half.

In order to examine the computational advantage of the MG procedure with increasing refinement of the finest grid, solutions were also obtained with a 41×41 finest grid. Figures 3a–3c show the resulting convergence history for p on plane 3 for three duct configurations. The MG procedure now uses a total of four grid levels. The corresponding convergence histories for the three-level MG procedure as well as the single-grid optimum SOR procedure are also included in each case. Table 2 shows the number of iterations and the CPU time required for the Φ and p solutions on planes 3 and 5. For plane 3 of the SSU configuration, the four-level MG-GS procedure leads to a fivefold reduction in the number of iterations as compared to the SG-optimum SOR scheme. The corresponding reduction factor is only about 3.5 with the three-level MG-GS scheme. For the CPS configuration, the reduction factor for the four-level MG-CS scheme is about 3. The asymptotic convergence rate, or the rate at which the L_2 norm of the residuals on the finest grid is reduced per multigrid cycle using four grid levels, is approximately 0.2 for the SSU configuration; this is comparable to the theoretical rate of 0.19 given by Brandt[6] for the Poisson equation on a uniform Cartesian mesh with Dirichlet boundary conditions. For the corresponding CPS configuration, using a clustered grid as shown in Fig. 4, a somewhat slower convergence rate of 0.38 was observed. The difference between this rate and the theoretical rate is not surprising, in view of the fact that the asymptotic convergence rate of 0.19 determined theoretically corresponds to a Dirichlet problem with constant coefficients. On the other hand, the CPS problem involves nonconstant coefficients and is a Neumann problem. In fact, the observed rate is expected to decrease with increase in degree of grid clustering, since that leads to more rapidly varying coefficients in the CPS problem.

For the results presented in Fig. 3 and Table 2, convergence was defined to occur when the L_2 norm of the residuals in the Poisson equation was below 7×10^{-7} for the SSU configuration and below 2×10^{-7} for the general CPS configurations. The corresponding values of the local relative error in the solution were approximately 10^{-10}.

Results for ADI Smoothing

The fact that, on single grids, implicit iterative schemes are more efficient than explicit schemes for elliptic boundary-

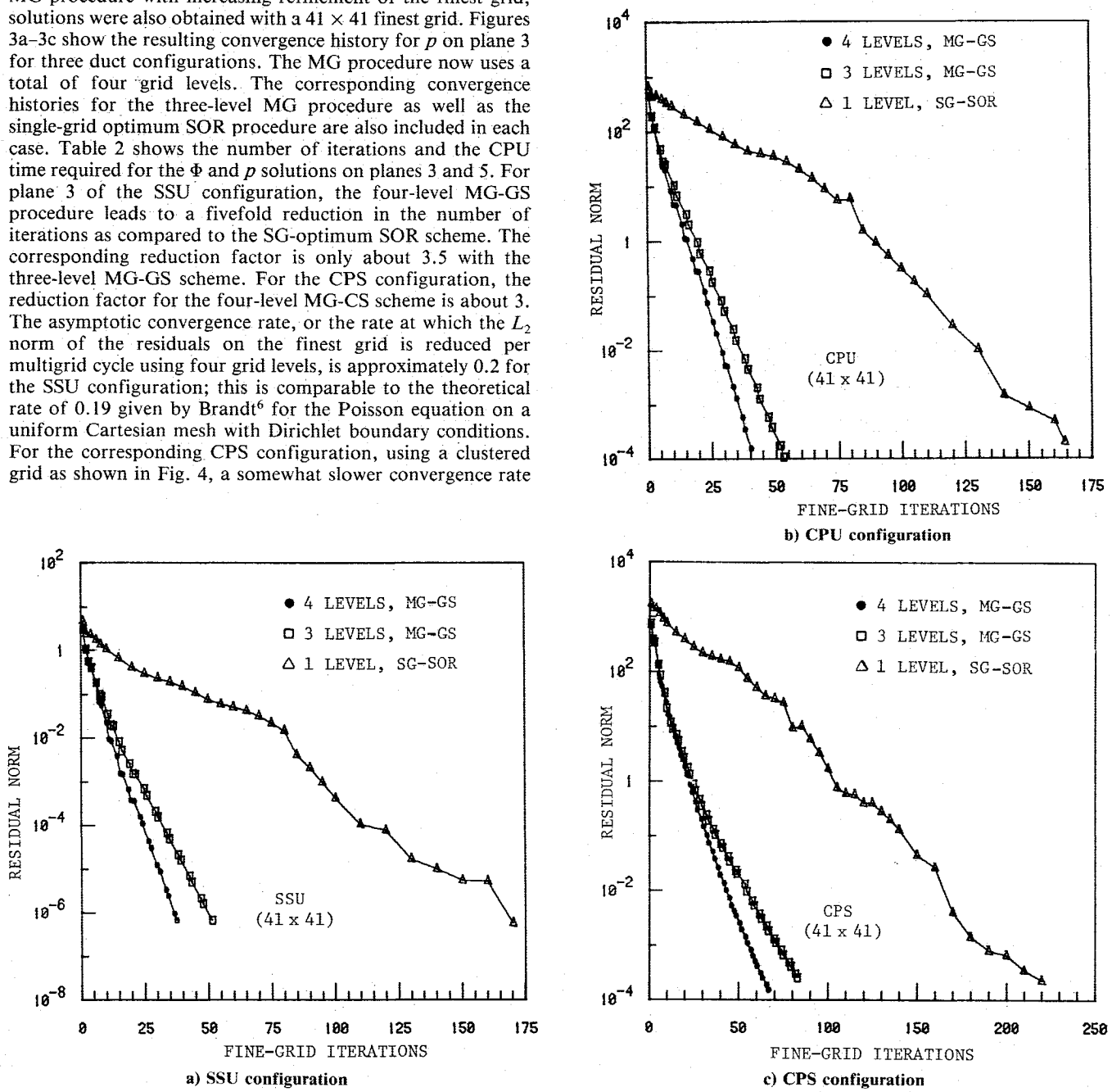

a) SSU configuration

b) CPU configuration

c) CPS configuration

Fig. 3 Convergence history for SOR and MG-GS schemes: p equation, plane 3.

Table 2 Comparison of computational effort for MG-GS and SG-SOR schemes: finest grid, 41 × 41

	Duct configuration	MG-GS – 4 levels				MG-GS – 3 levels				SG-SOR			
		Plane 3		Plane 5		Plane 3		Plane 5		Plane 3		Plane 5	
		Φ	p	Φ	p	Φ	p	Φ	p	Φ	p	Φ	p
No. of iterations	SSU	34.4	37.4	33.0	37.7	44.4	51.3	46.9	51.8	159	170	156	172
$t_{Poisson}$ CPU s		2.83	3.03	2.67	3.11	3.71	4.21	3.82	4.20	11.10	11.86	10.90	12.00
Remarks		$\zeta = 0.6$, $\delta = 0.3$				$\zeta = 0.6$, $\delta = 0.3$				$\omega = 1.90$			
No. of iterations	CPU	35.4	40.1	33.3	36.6	45.6	50.8	46.2	51.8	144	164	139	161
$t_{Poisson}$ CPU s		2.87	3.32	2.71	3.00	3.88	4.35	3.84	4.32	9.96	11.34	9.62	11.15
Remarks		$\zeta = 0.6$, $\delta = 0.3$				$\zeta = 0.6$, $\delta = 0.3$				$\omega = 1.90$			
No. of iterations	CPS	55.3	65.4	52.2	59.3	76.6	85.4	70.6	81.6	187	222	174	201
$t_{Poisson}$ CPU s		4.75	5.59	4.49	5.10	6.40	7.14	5.84	6.73	12.95	15.40	12.05	14.07
Remarks		$\zeta = 0.6$, $\delta^a_{2,1} = 0.5$ $\delta_{3,2} = \delta_{4,3} = 0.4$				$\zeta = 0.6$, $\delta = 0.4$				$\omega = 1.922$			

[a] $\delta_{k,k+1}$: switching criterion between grid levels k and $k + 1$.

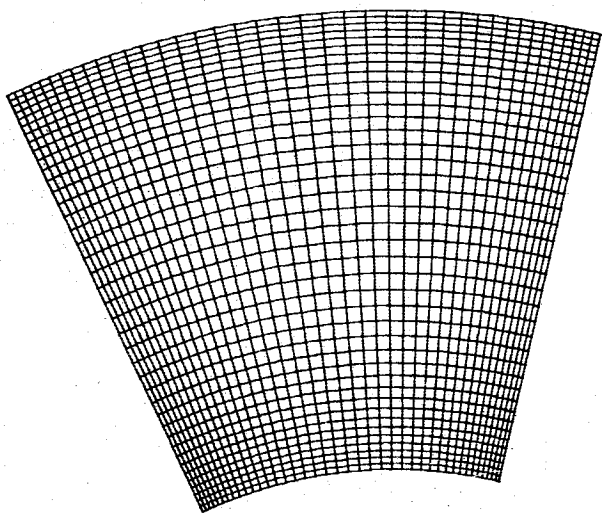

Fig. 4 Nonuniform 41 × 41 grid for polar configuration.

value problems suggested the use of an ADI scheme as the smoothing operator instead of the Gauss-Seidel scheme in the present MG procedure. This was also reinforced by the success that Jameson[12] has achieved with the MG-ADI scheme for transonic potential flows. In the present duct-flow analysis, the momentum equations are solved by the Douglas-Gunn[13] ADI procedure. Therefore, this ADI technique was implemented in the MG solution procedure also for the Φ and p equations. The details of the computational effort required for these solutions on planes 3 and 5 are summarized in Table 3. The present authors did not observe the insensitivity of the solution convergence rate to the value of Δt that was reported by Jameson.[12] Here, Δt is the fictitious time step required in formulating the ADI scheme. The optimum value of Δt is that which minimizes all the Fourier components of the error. For equations with nonconstant coefficients, e.g., for CPS configuration, the optimum Δt varies over the duct cross plane. Clearly, this evaluation is tedious at best, even when performed numerically. However, for Fourier components with wavelength equal to four or two times the grid interval, this evaluation is quite convenient. Therefore, for the results shown in Table 3, Δt was optimized with respect to these two error components and is indicated by subscripts $\pi/2$ and π. In comparison with the MG-GS results shown in Table 2, the MG-ADI scheme requires fewer iterations, but the computational time is almost the same. This is because one ADI iteration is more time consuming than one GS iteration. Similar observation was made by Ghia and Sokhey,[3] who employed the Peaceman-Rachford ADI scheme with a seven-

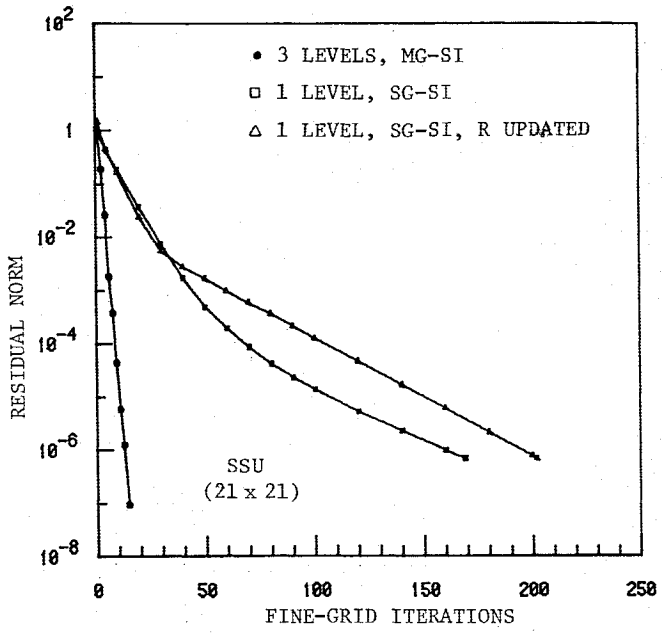

a) SSU configuration

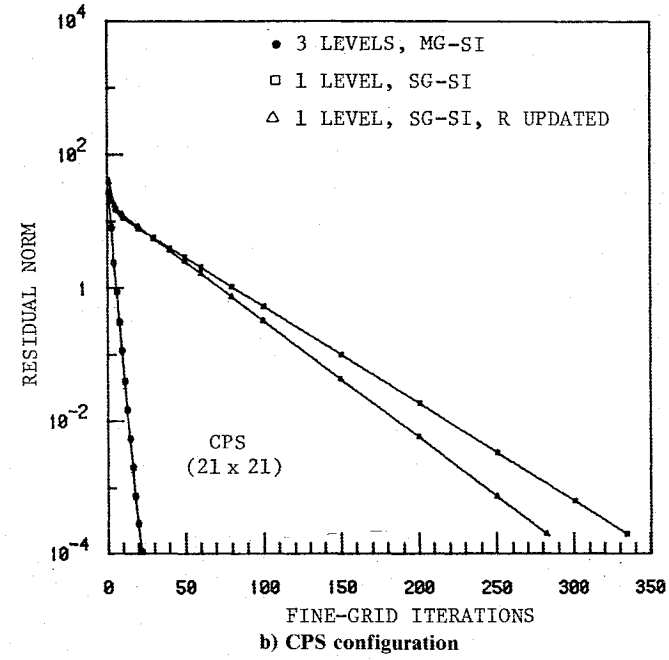

b) CPS configuration

Fig. 5 Convergence history for SI and MG-SI schemes: p equation, plane 3, 21 × 21 grid.

Table 3 Computational effort for MG-ADI scheme

	Duct configuration and finest grid	$\Delta t_{\pi/2}$ Plane 3 Φ	$\Delta t_{\pi/2}$ Plane 3 p	$\Delta t_{\pi/2}$ Plane 5 Φ	$\Delta t_{\pi/2}$ Plane 5 p	Δt_{π} Plane 3 Φ	Δt_{π} Plane 3 p	Δt_{π} Plane 5 Φ	Δt_{π} Plane 5 p
No. of iterations	SSU	12.81	12.81	11.13	12.81	16.19	19.56	16.19	16.19
$t_{Poisson}$ CPU s	(21 × 21)	0.583	0.581	0.509	0.587	0.738	0.893	0.741	0.746
No. of iterations	CPS	41.5	44.88			34.75	39.81		
$t_{Poisson}$ CPU s	(21 × 21)	1.908	2.068			1.619	1.858		
No. of iterations	SSU	32.76	34.44	31.10	34.44	16.05	17.70	17.70	16.05
$t_{Poisson}$ CPU s	(41 × 41)	5.33	5.57	5.03	5.60	2.60	2.87	2.86	2.60
No. of iterations	CPS	67.88	76.23	57.84	62.86	49.50	56.20	46.14	42.80
$t_{Poisson}$ CPU s	(41 × 41)	10.79	12.42	9.41	10.28	8.06	9.15	7.44	6.88

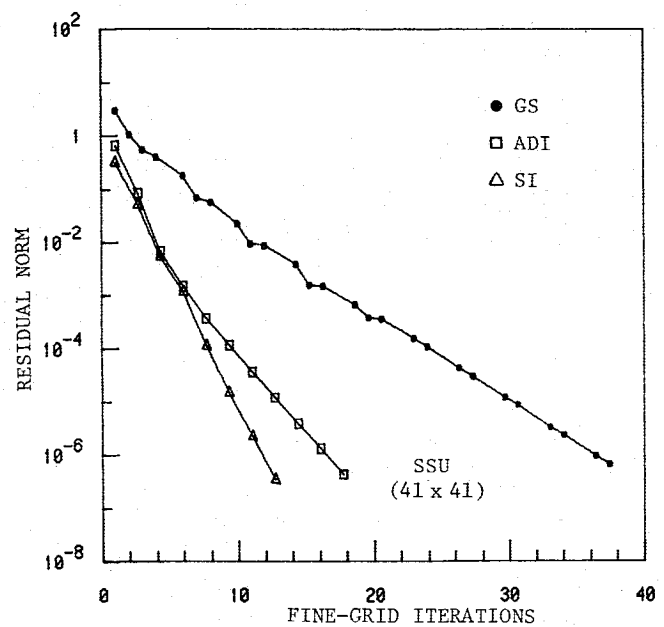

a) SSU configuration

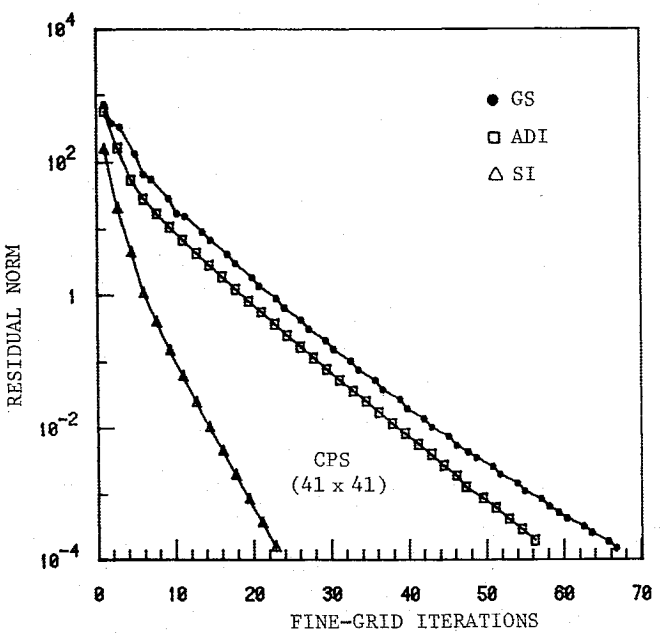

b) CPS configuration

Fig. 6 Comparative study for multigrid schemes using various smoothing operators: p equation, plane 3.

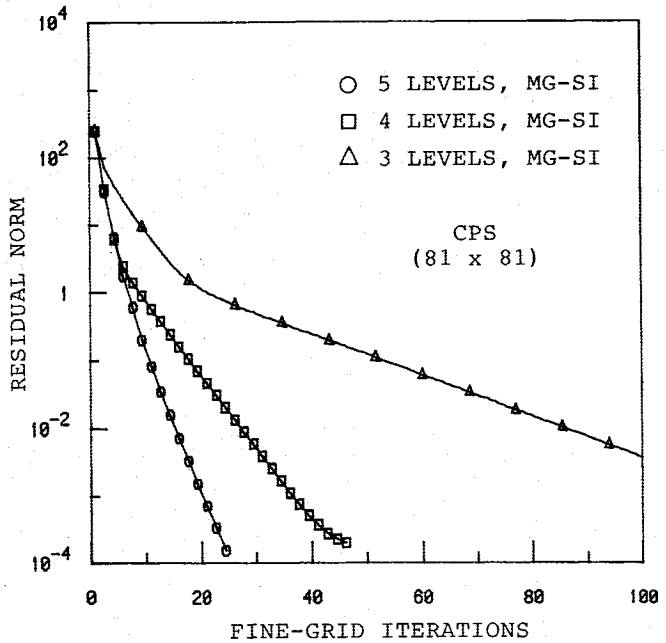

Fig. 7 Convergence history for MG-SI scheme: p equation, plane 3, 81 × 81 grid.

parameter optimum sequence for Δt to solve the Φ and p equations. For the SSU configuration, Ghia and Sokhey[3] reported convergence of their single-grid solutions in 34 iterations for the Φ equation, with convergence defined as relative error below 10^{-8}. In the present MG-ADI procedure, this level of convergence is achieved in about 13 iterations for the same case.

With the ADI scheme, both adaptive and fixed MG algorithms were studied from the viewpoint of overall efficiency. Unlike the adaptive MG-GS scheme, the adaptive MG-ADI scheme was found to be rather sensitive to the values of δ used for switching between two successive grid levels. Hence, the adaptive MG-ADI procedure was not pursued much further. The results in Table 3 correspond to the fixed MG algorithm consisting of one iteration on each grid except the coarsest, on which three iterations were performed.

Results for SI Smoothing

Since the ADI scheme continued to remain sensitive to the parameter Δt even when used in conjunction with the MG scheme, effort was directed to the use of the SI scheme as the smoothing operator. First proposed by Stone[14] and later extended by Rubin and Khosla,[15] the SI scheme is relatively insensitive to the value of Δt. Its adaptation for use with the

Table 4 Comparison of computational effort for MG-SI and SG-SI schemes: finest grid, 21 × 21

	Duct configuration	MG-SI – 3 levels				SG-SI			
		Plane 3		Plane 5		Plane 3		Plane 5	
		Φ	p	Φ	p	Φ	p	Φ	p
No. of iterations	SSU	12.81	14.5	11.13	12.81	126	159	104	133
$t_{Poisson}$ CPU s	SSU	0.407	0.468	0.356	0.406	3.480	4.400	2.870	3.670
No. of iterations	CPS	17.88	21.25	16.19	17.88	279	334	252	294
$t_{Poisson}$ CPU s	CPS	0.585	0.702	0.528	0.580	7.500	9.000	6.820	7.990

present Neumann problem required considerable reformulation of the various recursion relations involved at the boundaries. All boundary conditions were treated implicitly and with second-order accuracy. The scheme was then used, with $\Delta t \to \infty$, in conjunction with a fixed MG procedure. The resulting convergence history for the solution for p on plane 3 is shown in Fig. 5 for the SSU and the CPS configurations for the 21×21 grid. Included in Fig. 5 are the corresponding curves for the SG-SI solutions and those for the SG-successive SI scheme[16] in which one of the recursion coefficients is updated during the back-substitution step of the procedure. The advantages of using the MG procedure are seen clearly in Fig. 5. It is not clear why the successive SI scheme is less efficient than the SI scheme for the SSU configuration; this point needs to be examined further.

Table 4 provides some additional computational information for the MG-SI procedure and the SG-SI procedure. As compared to the latter, the MG-SI scheme provides a tenfold reduction in the number of iterations for the SSU configuration. The corresponding reduction factor is 15 for the CPS configuration. It is observed that the number of iterations required on plane 3 by the SG-SI scheme is two to three times that of the SG-SOR scheme, as seen from Tables 1 and 4. The main reason for this is that the relaxation factor for the single grid was optimized for the SOR scheme and not for the SI scheme.

The present study enables comparison of the three smoothing operators employed in the MG procedure. Figure 6 shows the convergence history for the p solution on plane 3 for the MG scheme with the three smoothing procedures used. For the SSU and the CPS configurations, the SI smoothing provides the fastest convergence, whereas GS smoothing contributes to the slowest convergence of the MG scheme. For the SSU case, the MG-ADI curve is nearer to the MG-SI curve, whereas for the CPS case, it shifts close to the MG-GS curve. This again illustrates the sensitivity of the ADI scheme to the parameters of the problem.

Finally, Fig. 7 shows the convergence history for the p solution on plane 3 employing a clustered grid with 81×81 points. It is clear that the five-level MG-SI scheme leads to a twofold reduction in the number of iterations, when compared to a four-level scheme, and almost a fourfold reduction as compared to a three-level scheme. Convergence is achieved in approximately 25 iterations using the five-level MG-SI scheme. Figures 6 and 7 also demonstrate that the number of iterations required for convergence remains approximately the same as the grid is refined, i.e., the MG-SI scheme is almost insensitive to grid refinement. With respect to defining convergence, Ramamurti[17] has shown that the relation between the L_2 norm of the residuals and other forms of measuring convergence based on relative error is almost linear and that the convergence criterion based on the residual norm is the most stringent.

VI. Conclusion

The multigrid technique has been studied further for use with the generalized Neumann boundary-value problem in curvilinear coordinates with grid-clustering transformations. The restriction operator R_k^{k-1} at interior points, boundary points, and corner points has been formulated appropriately to satisfy the discretized representation of the integral constraint associated with Neumann problems. The coefficients in the differential operators for the coarse-grid correction equation are formulated using this restriction operator to satisfy the divergence theorem. Results have been obtained for the Neumann problems encountered in parabolic-flow analysis of various duct configurations.

Comparison of the MG solution convergence history of single-grid solutions confirms again the computational advantage of the MG technique. The relaxation scheme used in the MG procedure is observed to influence the efficiency of the overall scheme. The GS smoother performs quite well, but the SI scheme contributes to greater efficiency, whereas the ADI scheme continues to remain sensitive to the iteration parameters.

This study provides an important step in the solution of Navier-Stokes equations using the velocity-pressure formulation. Effort is presently continuing toward obtaining finer-mesh results for the entire developing flow through various duct configurations.

Acknowledgments

This research was supported in part by AFOSR Grant 80-0160 and in part by NASA Grant NSG 3267.

References

[1]Ghia K. N., Hankey, W. L., and Hodge, J. K., "Study of Incompressible Navier-Stokes Equations in Primitive Variables Using Implicit Numerical Technique," *AIAA Journal*, Vol. 17, March 1979, pp. 298–301.

[2]Briley, W. R., "Numerical Method for Predicting Three Dimensional Flows in Ducts," *Journal of Computational Physics*, Vol. 14, Jan. 1974, pp. 8–28.

[3]Ghia, K. N. and Sokhey, J. S., "Laminar Incompressible Viscous Flow in Curved Ducts of Regular Cross-Sections," *Journal of Fluids Engineering*, Vol. 99, No. 4, Dec. 1977, pp. 640–648.

[4]Ghia, U., Ghia, K. N., and Struderus, C. J., "Three Dimensional Laminar Incompressible Flow in Straight Polar Ducts," *International Journal of Computers and Fluids*, Vol. 5, No. 4, Dec. 1977, pp. 205–218.

[5]Ghia, U., Ghia, K. N., and Goyal, R. K., "Three-Dimensional Viscous Incompressible Flow in Curved Polar Ducts," AIAA Paper 79-1536, July 1979.

[6]Brandt, A., "Multi-Level Adaptive Computations in Fluid Dynamics," AIAA Paper 79-1455, July 1979.

[7]Ghia, K. N., Ghia, U., Shin, C. T., and Reddy, D. R., "Multi-Grid Simulation of Asymptotic Curved-Duct Flows Using a Semi-Implicit Numerical Technique," *Computers in Flow Predictions and Fluid Dynamics Experiments*, edited by K. N. Ghia, T. J. Mueller, and B. R. Patel, American Society of Mechanical Engineers, New York, 1981.

[8]Ghia, U., Ghia, K. N., and Shin, C. T., "High-*Re* Solutions for Incompressible Flow Using the Navier-Stokes Equations and a Multi-Grid Method," *Journal of Computational Physics*, Vol. 48, No. 3, Dec. 1982, pp. 387–411.

[9]Ghia, U., Ghia, K. N., and Ramamurti, R., "Multi-Grid Solution of Neumann Pressure Problem for Viscous Flows Using Primitive Variables," AIAA Paper 83-0557, Jan. 1983.

[10]Goyal, R. K., Ghia, K. N., and Ghia, U., "Numerical Simulation of Three-Dimensional Turbulent Flow in Curved Ducts Using Parabolized Navier-Stokes Equations," 3rd International Conf. on Mathematical Modelling, Los Angeles, CA, July 1981.

[11]Wesseling, P., "Theoretical and Practical Aspects of a Multi-Grid Method," Delft Univ. of Technology, Delft, the Netherlands, Rept. NA-37, 1980.

[12]Jameson, A., "Acceleration of Transonic Potential Flow Calculations on Arbitrary Meshes by Multiple Grid Method," AIAA CP-799, July 1979, pp. 147–156.

[13]Douglas, J. and Gunn, J. E., "The ADI Methods for Parabolic and Hyperbolic Equations," *Numerishe Mathematik*, Vol. 6, No. 5, Dec. 1964, pp. 428–453.

[14]Stone, H. L., "Iterative Solution of Approximations of Multi-Dimensional Partial Differential Equations," *SIAM Journal of Numerical Analysis*, Vol. 5, No. 3, Sept. 1968, pp. 530–559.

[15]Rubin, S. G. and Khosla, P. K., "Navier-Stokes Calculations with a Coupled Strongly Implicit Method – I: Finite Difference Solutions," *International Journal of Computers and Fluids*, Vol. 9, No. 2, June 1981, pp. 163–180.

[16]Rubin, S. G., "Incompressible Navier-Stokes and Parbolized Navier-Stokes Solution Procedures and Computational Techniques," Lecture Notes, von Kármán Institute, Brussels, Belgium, 1982.

[17]Ramamurti, R., "Multi-Grid Solution of Neumann Problems in Simulation of Viscous Flows in Ducts," M.S. Thesis, Univ. of Cincinnati, OH, 1983.